

Dimensionality Variation in Polymeric Metallo-Organic Frameworks

Kalle I. Nättinen,^[a] Juha Linnanto,^[a] and Kari Rissanen*^[a]**Keywords:** Crystal engineering / X-ray diffraction / Self-assembly / Coordination polymers

Single crystal X-ray crystallography was used to determine the structures of four metallo-organic complexes derived from pyridyl ligands and the metal ions, Cu²⁺, Zn²⁺ and Ag⁺. Two metallo-organic layer framework structures (**1** and **3**), a strand (**2**) and a dimer (**4**) structure were formed when the tetradentate ligands, tetrakis(nicotinoxymethyl)methane (TNM) and tetrakis(isonicotinoxymethyl)methane (TINM), were reacted with the first and second row transition metal cations, copper, silver, and zinc. The choice of anion and ligand was found to affect the outcome of the structure. Contrary to our previous results with the same ligands and similar transition metal cations, no genuine 3D metallo-organic frameworks (MOFs) were obtained. Several factors were found to affect MOF formation: the coordination geometry, the *meta*- or *para*-configuration of the coordinating pyridyl moieties and the size and type of the counter anion. In **1**, the

use of TNM (with a shorter "coordination arm" than TINM), in combination with an octahedral coordination geometry (4 Py, SO₄²⁻ and H₂O) and a relatively large sulfate anion, leads to a sandwich-like layer structure with the anions between the MOF layers. The layers have a thickness of 2.1 nm. In complex **3**, similar layer structures are assembled from four- and five-coordinate (2 Py, NO₃⁻, H₂O/2 Py, 3 NO₃⁻) Ag⁺ ions with TINM and nitrate anions. However, in complex **2**, the Zn²⁺ ion is tetrahedrally (2 Py, 2 Cl⁻) coordinated, creating an infinite strand structure. Most surprisingly, in complex **4**, two arms of the ligand are uncoordinated and a binuclear square-planar coordination geometry (2 Py, 2 CH₃COO⁻) around the Cu²⁺ ions, as well as the acetate anions, create a non-polymeric dimeric structure.
(© Wiley-VCH Verlag GmbH & Co. KGaA, 69451 Weinheim, Germany, 2003)

Introduction

The ease with which new polymeric metallo-organic materials can be analyzed and synthesized, as well as their potential capacity for a range of applications, have in the last decade created an interesting field of chemistry dealing with supramolecular, polymeric strands, sheets, and 3D networks. Possible applications include trapping (or clathrating) of guest molecules,^[1] chemical sensing,^[2] light element ceramics,^[3] electronic switches, and gas-storage.^[4,5] Molecular self-assembly enables the synthesis of these complexes by the utilization of molecular tectons^[6] and supramolecular synthons^[7] to create infinite polymers that form crystals. The tectons are held together by a variety of interactions such as metal–ligand coordination bonds,^[8–11] hydrogen-bonds,^[12–15] stacking interactions,^[16] S–S bonds,^[11] metal-metal contacts,^[17] weak hydrogen–bonds,^[16,18] $\pi\cdots\pi$ interactions or mixtures of these.^[9,19] The networks created from the tectons come in many forms such as one-dimensional rods, ladders and tubes,^[20] two-dimensional grids, sheets or honeycombs,^[9] three-dimensional diamondoid (tetrahedral centers),^[12,17,21,22] or simple cubic lattices (octahedral

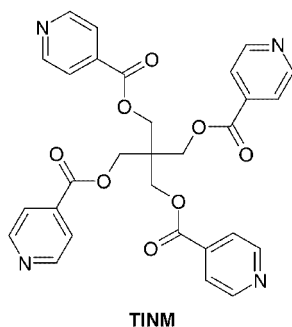
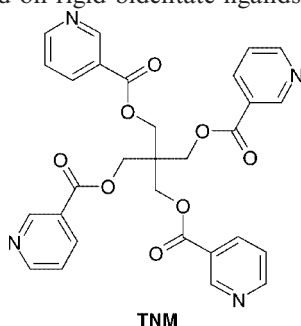
centers).^[23–25] The coordination networks offer some attractive properties which include modularity (i.e. the availability of a large number of identical sites), regioselectivity, stereoselectivity, shape selectivity, and exact information on the nature of binding (i.e. position in the crystal lattice), as opposed to absorption or adsorption on the surface.^[26] Although crystal engineers try to control the properties of the crystal,^[27] the majority of crystallizations lead to unexpected results, such as the formation of two different structures from one crystallization method,^[8] or the formation of different MOFs from the *cis*- and *trans*-isomers of a ligand.^[28]

We have previously studied the interpenetrating 3D MOFs formed by TINM and the first row transition metal cations, copper, nickel and cobalt.^[29] This work deals with metallo-organic complexes that form architectures with fewer dimensions than the MOFs studied in our previous work. Despite some examples of tetradentate ligands used in the synthesis of one- or two-dimensional structures, most of the structures are synthesized from bidentate ligands, such as 4,4'-bipyridine, or tridentate ligands.^[17,23,30–32] This is partly due to ease with which the starting materials for the bidentate MOFs are synthesized, and the fact that the tetrahedral conformation typical of tetradentate MOFs tend to lead to 3D networks.^[29,33] In this work, we investigate the effect of using the *meta*- (TNM) and *para*-isomers (TINM) of the same ligand with a selection of anions and the first and second row transition metal cations, copper, zinc, and silver. The effects on MOF formation, and on the

^[a] Department of Chemistry, University of Jyväskylä,
P. O. Box 35, 40351 Jyväskylä, Finland
E-mail: Kalle.Nattinen@cc.jyu.fi
juha.linnanto@c.c.jyu.fi
Kari.Rissanen@cc.jyu.fi

Supporting information for this article is available on the WWW under <http://www.eurjic.org> or from the author.

geometry and dimensions of the formed frameworks were investigated. The use of flexible organic ligands adds an element of freedom to the coordination geometry of the metal atoms. Therefore, one would expect a deviation from the structures based on rigid bidentate ligands.



Results and Discussion

Synthesis: X-ray quality crystalline solids of complexes **1–4** were obtained by evaporation of the solvents. All combinations of the ligands, TNM and TINM, and the metal salts, copper diacetate, copper- and silver nitrate, zinc, cobalt, and nickel chloride, and copper sulfate, and the solvents and solvents mixtures, MeOH, MeCN, CH₂Cl₂, and H₂O, were tried. Almost all the complexation attempts produced fine microcrystalline precipitates. Complexes **1–4** were the only single crystalline solids that could be collected. The structures were further confirmed using elemental analysis and TGA. Since complexes **1–4** only exist as solid crystalline material, no NMR measurements were performed.

X-ray Single Crystal Structures

The crystal data for complexes **1–4** are presented in the Table 1. No unusual metal coordination angles or bond lengths were found in the structures.

Layer Structure 1: The asymmetric unit of **1** consists of half a molecule of TNM, with skewed tetrahedral coordination of the arms, one copper cation, one coordinated disordered sulfate anion, five water molecules, and one methanol molecule. A model to describe the sulfate disorder was built by splitting the sulfate molecule into two positions. Two water molecule halves were located in special positions, two were disordered to two and three positions, respectively.

Table 1. Crystallographic parameters for complexes **1–4**

Complex	1	2	3	4
Empirical formula	[Cu(C ₂₉ H ₂₄ N ₄ O ₈)(SO ₄)(H ₂ O) ₂ ·(CH ₃ OH) ₂ (H ₂ O) ₈] ^[a]	[Zn ₂ (C ₂₉ H ₂₄ N ₄ O ₈)Cl ₄ ·(CH ₃ CN) _{2/3} (H ₂ O) _{1/3}]	[Ag ₂ (C ₂₉ H ₂₄ N ₄ O ₈ ·(NO ₃) ₂ (H ₂ O)]	[Cu(C ₂₉ H ₂₄ N ₄ O ₈ ·(O ₂ CCH ₃) ₂ (H ₂ O) ₄]
Formula mass	952.30	855.74	914.30	810.22
Crystal color, shape	blue, plates	yellow, blocks	colorless, blocks	blue, prisms
Crystal dimensions (mm)	0.08 × 0.2 × 0.3	0.15 × 0.15 × 0.3	0.20 × 0.25 × 0.4	0.08 × 0.15 × 0.5
Crystal system	Monoclinic	Trigonal	triclinic	triclinic
Space group	<i>P</i> 2 ₁ / <i>c</i> (No.13)	<i>P</i> 3(2) ₁ (No.154)	<i>P</i> 1̄ No.2	<i>P</i> 1̄ (No.2)
<i>a</i> (Å)	10.5626(4)	12.511(2)	9.1111(2)	10.8279(4)
<i>b</i> (Å)	15.3884(6)	12.511(2)	11.1364(2)	10.8228(4)
<i>c</i> (Å)	13.7398(5)	21.472(4)	15.4384(4)	18.7422(9)
α (°)	90	90	91.057(1)	77.639(2)
β (°)	100.219(2)	90	90.350(1)	74.946(2)
γ (°)	90	120	90.218(2)	60.785(2)
<i>V</i> (Å ³)	2197.9(2)	2910.6(9)	1566.15(6)	1841.2(2)
Calcd. density (Mg/m ³)	1.439	1.465	1.939	1.461
Temp. during data collection (K)	173	173	173	173
<i>Z</i>	2	3	2	2
<i>R</i> _{obsd.}	<i>R</i> 1 = 0.0642, <i>wR</i> 2 = 0.1678	<i>R</i> 1 = 0.0362, <i>wR</i> 2 = 0.0998	<i>R</i> 1 = 0.0302, <i>wR</i> 2 = 0.0677	<i>R</i> 1 = 0.0560, <i>wR</i> 2 = 0.1244
<i>R</i> _{all}	<i>R</i> 1 = 0.0891, <i>wR</i> 2 = 0.1861	<i>R</i> 1 = 0.0429, <i>wR</i> 2 = 0.1039	<i>R</i> 1 = 0.0382, <i>wR</i> 2 = 0.0708	<i>R</i> 1 = 0.0835, <i>wR</i> 2 = 0.1363
GooF	1.060	1.128	1.082	1.075
θ range for data collection (°)	2.98 to 25.69	3.26 to 25.02	2.24 to 25.00	3.29 to 25.70
Scan type	Φ/Ω , 2°	Φ/Ω , 2°	Φ/Ω , 2°	Φ/Ω , 1°
Refl. collected/unique/cell refinement	14322/4313/4010	29711/10200/9491	14486/5488/5006	11447/6830/5779
Refined parameters	372	225	475	513
Residual electron density e/Å ³	0.611/−0.686	0.738/−0.229	0.402/−0.518	0.858/−0.576
min./max. abs. correction	0.8902/0.9407	0.7397/0.7753	0.7304/0.7489	—

^[a] The hydrogens could not be located for all the water and methanol molecules.

Hydrogen atoms could not be located for the disordered water molecules. The TNM ligand is coordinated by the copper cations through the four aromatic nitrogen atoms. The coordination geometry around the copper atom is octahedral.

A schematic presentation of the ligand and its surroundings in complex **1** is displayed in Scheme 1. The 2D MOF of **1** is a grid that is puckered so that the equatorial copper coordination planes are placed both on top and bottom of the layer that is formed. The TNM ligands form the inside of the layer. The equatorial coordination bonds of the copper atoms are coplanar with the layer. Therefore, all the arms of TNM are directed towards center of the layer (Figure 1). The puckering arises as a result of the *meta*-position of the nitrogen atom of TNM and the relatively large size of the sulfate anion. The puckered structure results in the formation of open channels on top and bottom of the layers. The channels are filled by water molecules and occupied by sulfate anions from the neighboring layer (Figure 2).

In our previous work we synthesized two complexes of TINM with copper nitrate.^[29] Both of these complexes are two-fold interpenetrating 3D MOF structures with channels formed by cavities that contain nitrate anions and solvent water molecules. The “effective” length (distance between central carbon atom and the coordinating nitrogen atom) of the TINM ligand is longer than that of the TNM ligand. The nitrate anion is also smaller than the sulfate anion. In addition, with the nitrogen atom in the *meta*-position of TNM, the arms of the ligand cannot be straightened so as to satisfy the square-planar coordination geometry around the copper cation. Due to the distorted tetrahedral conformation of the arms, combined with the *meta*-position of the aromatic nitrogen atom, complex **1** forms a pseudo 3D MOF that does not elongate infinitely in all dimensions, but instead creates thick layers perpendicular to the crystallographic *b*-axis. Therefore, it is not a true 3D MOF in this respect. However, its third dimension is in the nanoscale range: the thickness of the layers is 2.1 nm.

In order to provide enough space for the sulfate anion, the structural components of **1** should create a non-interpenetrating MOF rather than the two-fold interpenetrating MOF previously observed with $\text{Cu}(\text{NO}_3)_2$ and TINM.^[29] However, the difference in the size of the anions is probably not enough to allow for the formation of a stable non-interpenetrating MOF: the sulfate anions are not large enough to support the formation of a framework that would not collapse without a second interpenetrating framework. We have performed molecular modeling, the results of which support this hypothesis. The channels contain water molecules with hydrogen atoms pointed towards the highly negative electron potential of the sulfate anions. The negative electron potential of the sulfate anion requires too much space for the 3D network to be formed. All attempts to crystallize a 3D MOF from TNM and a metal cation with octahedral coordination (Cu, Ni, Co) failed, thereby also supporting the spatial and conformational requirements of the TNM ligand.

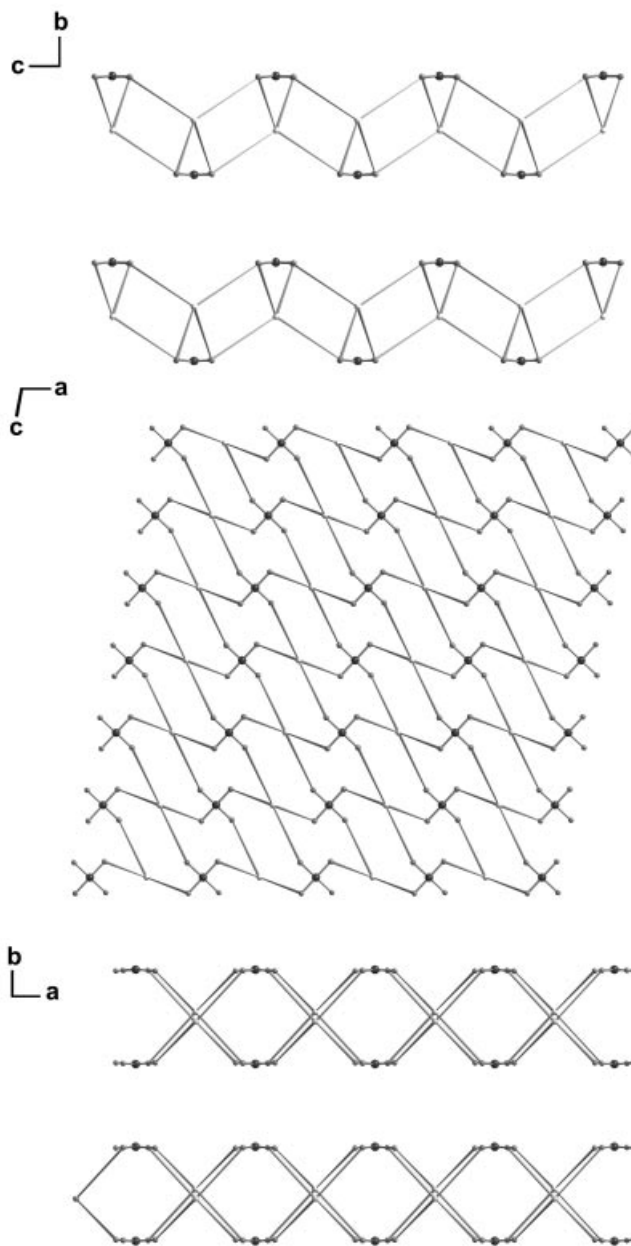


Figure 1. A view of the ball-and-stick model of two layers of **1** along the crystallographic unit cell axes *a*, *b*, and *c*. Only the central carbon atoms, terminal nitrogen atoms of TNM, the copper atoms, and the bonds between them are shown. The separation between the two layers is 3.5 Å

Strand Structure 2: The asymmetric unit of **2** consists of a Zn atom, half a molecule of TNM coordinated by it, two chloride anions coordinated by the zinc atom, a water molecule, and an acetonitrile molecule. The water molecule is situated in a special position and was located with a population parameter 1/2 and a site occupancy of 1/3. The terminal carbon atom of the acetonitrile molecule is also in a special position. The acetonitrile was located with a population parameter 1/2 (besides the terminal carbon atom for which a population parameter 1/2 and a site occupancy of 1/3 were applied). The solvent molecules are located inside

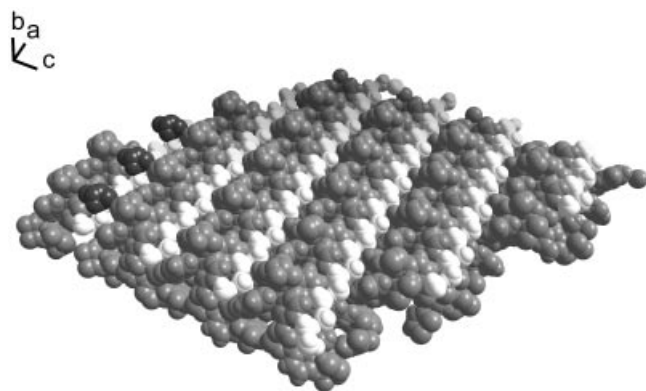
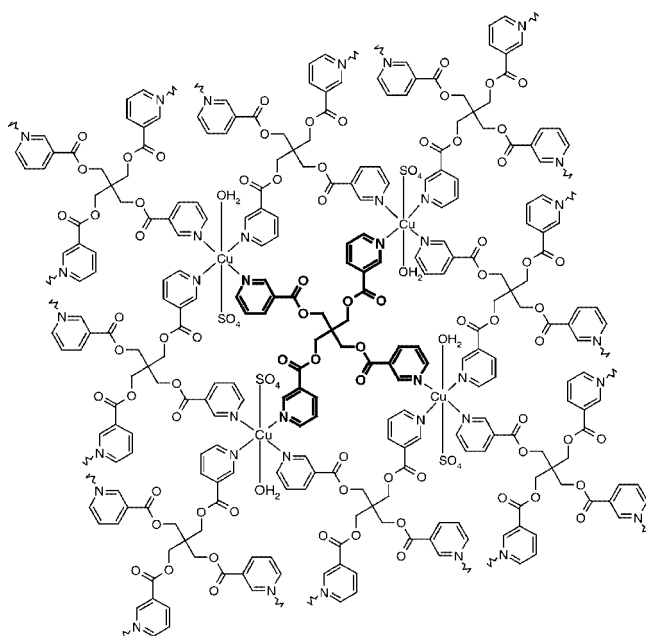


Figure 2. A perspective view of the space-filling model of a square section of the layer in **1**. The oxygen atoms of the water molecules are shown. The sulfate anions of the neighboring layer are displayed on top of the leftmost channel

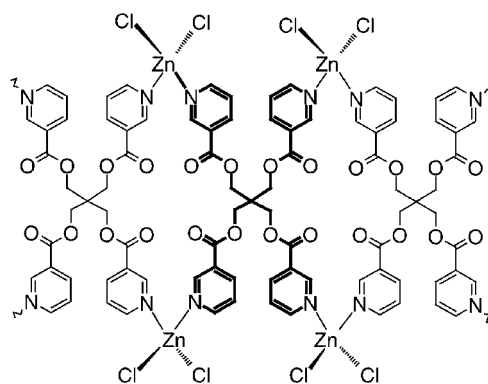


Scheme 1. A schematic representation of the layer network of **1**, with the central ligand shown in bold font

the cavity formed by the links of the chains. The coordination geometry around the zinc atom is tetrahedral.

A schematic representation of a polymeric unit of **2** is presented in Scheme 2. Due to the trigonal symmetry of the structure, each layer of stacked chains forms a 60° angle with those above and below it. The layers are formed perpendicular to the crystallographic *c*-axis (Figure 3).

The formation of a 3D MOF is prevented by two factors: the zinc cation has only two available coordination sites from its tetrahedral coordination sphere for the TNM ligand, and the arms of TNM are paired, i.e. their orientation is not tetrahedral. Therefore, the polymeric structure only grows in one dimension and there are no coordination bonds between individual chains (Scheme 2). Additionally, the chloride anion is not able to act as a bridging anion between two adjacent Cu centers, unlike the acetate or nitrate anions. The planar, cross-like conformation of the li-



Scheme 2. A schematic representation of **2**, with the central ligand shown in bold font

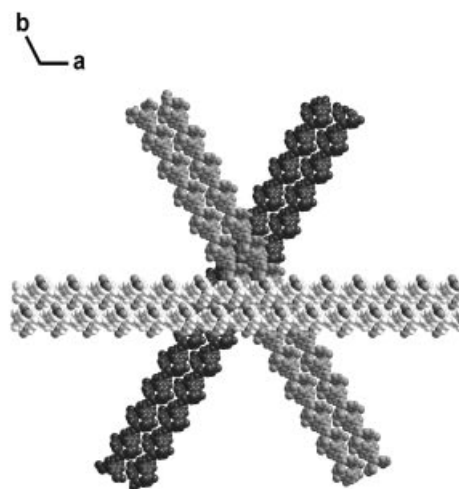


Figure 3. Two chains from each of the three layers with a unique orientation in complex **2** (the planes of the layers are in the plane of the paper). The orientation of the fourth layer is identical to that of the first layer. The chain pairs are displayed with the color intensity increasing along the *c*-axis. The solvent molecules are excluded

gand arms could create a 2D MOF, with four ligands forming one large square in the grid. This type of structure would probably need to be interpenetrated so as to stabilize the framework. However, only the strand structure **2** could be obtained from the complexation experiments. A probable explanation for not obtaining the 2D layer MOF is the high complementarity requirements of interpenetrating frameworks in the solid state. In our experiments, interpenetration was not observed in the single crystals that were obtained.

Layer Structure 3: The asymmetric unit of **3** consists of a non-tetrahedral TINM ligand that is coordinated to four silver cations, two of which belong to the asymmetric unit. There are also two nitrate anions and one water molecule that are coordinated to the silver cations. A plot with thermal ellipsoids of structure **3** is presented in Figure 4. The linear conformation of TINM is stabilized by $\pi \cdots \pi$ interactions between the pyridine rings C36–C41 and C26–C31 (separation between the centroids of the rings is 3.89 Å), as well as $\text{CH} \cdots \pi$ interactions between the remaining two arms [$d = 2.72$ Å for C17–H17 \cdots centroid (C6–C11)]. The $\pi \cdots \pi$

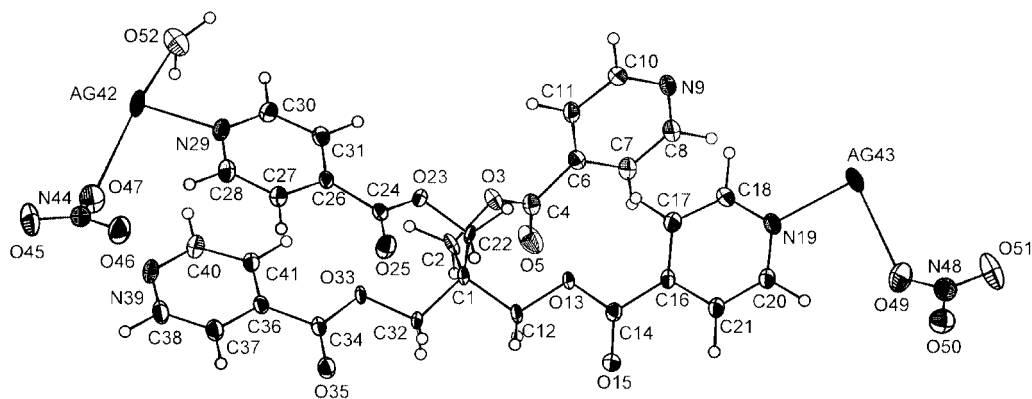
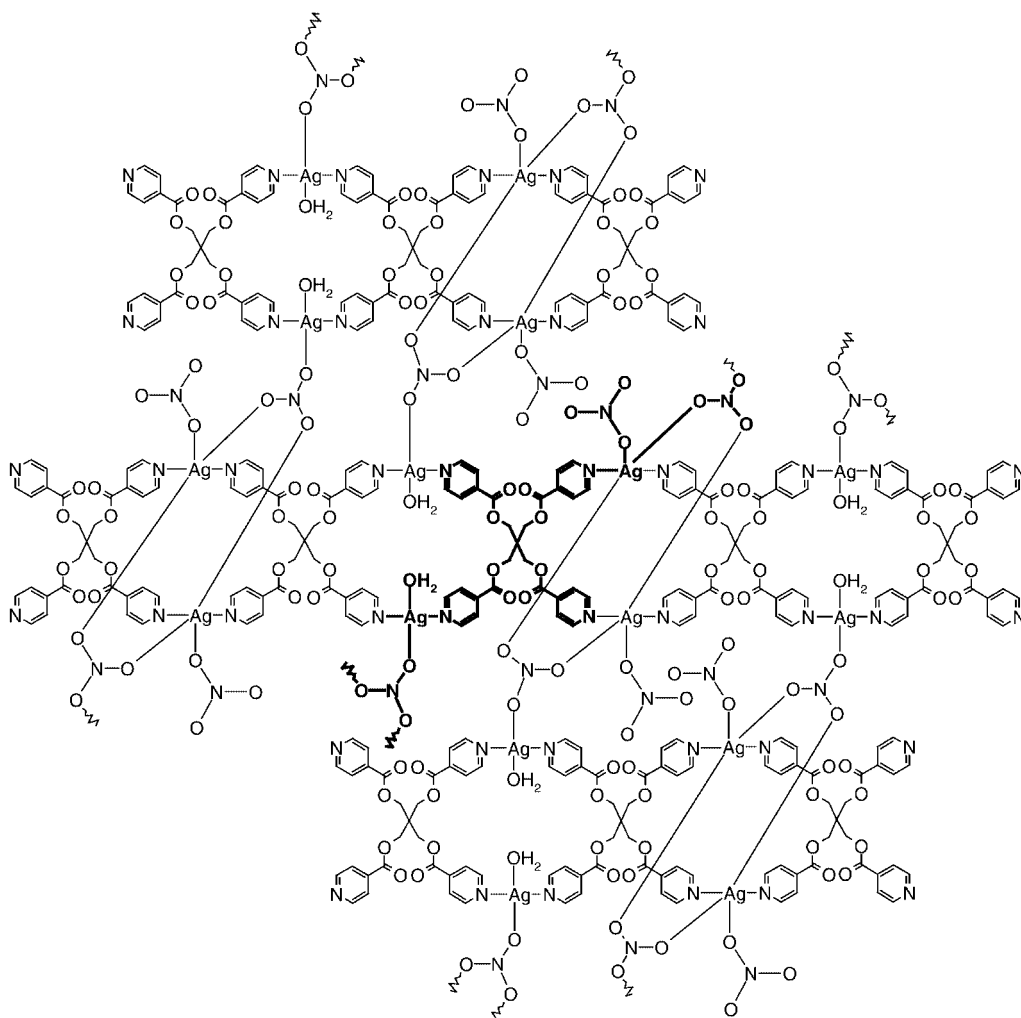


Figure 4. A plot with thermal ellipsoids shown at the 50% probability level for **3**. The non-hydrogen atoms of the asymmetric unit are numbered

interactions between the aromatic rings are attractive forces that bring the Ag^+ cations closer (within a distance of 4.07 Å from each other).

A schematic representation of the structure of **3** is displayed in Scheme 3. The neighboring chains provide additional nitrate anions for coordination by the Ag^+ cations.

This coordination creates additional connections in another direction of the lattice, thus forming a link between the chains of **3**, and leading to the formation of 2D layers (Figure 5) with a thickness of 13.2 Å. One silver cation (Ag42) exhibits a distorted square-planar coordination geometry, while the other (Ag43) exhibits a square-pyramidal ge-



Scheme 3. A schematic representation of the structure of **3**. The central asymmetric unit is shown in bold font. The chains run in a horizontal direction

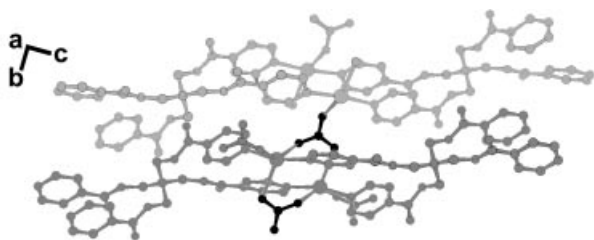


Figure 5. The links between the chains of **3**. Four TINM ligands and silver cations are shown. The different chains are shown in light and medium gray. For clarity, the bridging nitrate anions are shown in black ink and the hydrogen atoms are omitted

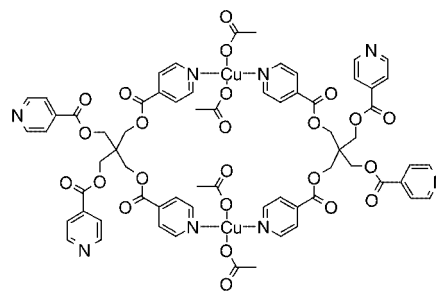
ometry. The two symmetry equivalent Ag43 cations are bridged by two nitrate anions (N44–O47 and its symmetry equivalent). They are also bridged to the neighboring chain Ag42 cations by the same nitrate anions, through the remaining oxygen atom of the nitrate anions. The other nitrate anion coordinated to the Ag43 cation does not form a bridge.

With the planar, cross-like conformation of the ligand arms, a 2D grid-like MOF could hypothetically be created by N–Ag bonds alone (see discussion of complex **2**). Anion coordination between layers could extend this structure into a 3D MOF, assuming that the anions would be suitably positioned. However, neither of these structures are observed. As with complex **2**, the probable explanation for not obtaining the 2D MOF is the high complementarity requirements of the interpenetrating frameworks. These requirements were not met by any quantitative combination of the TINM ligand and silver nitrate, since the layer structure **3** was the only single crystalline material that could be obtained. Since the arms of the TINM are paired, thereby providing an extension of the structure only in one dimen-

sion, the structure remains as a stack of anion-bridged 2D layers.

The three bond lengths involving the bridging nitrate anion are both shorter [Ag43–O46: 2.608(1) Å] and longer [Ag42–O47: 2.797(3) Å and Ag43–O45: 3.025(2) Å] than the bond length of the singly coordinated nitrate anion [Ag43–O49 of 2.651(1) Å]. The layers of **3** stack along the crystallographic *a*-axis, forming a dense lattice with no voids.

Dimeric Structure 4: Each asymmetric unit of **4** contains one Cu atom, one TINM ligand coordinated by the copper atom, two coordinated acetate anions and four water molecules. The four water molecules are hydrogen-bonded to the carbonyl oxygen atoms of the acetate anions or to those of the TINM core, except one, which is hydrogen-bonded to one of the water molecules. The coordination geometry around the copper atom is square-planar (Figure 6). The formation of dimers and the $\pi\cdots\pi$ interactions between the pyridine rings (3.66 Å between the centroids) of parallel arms (as in **3**) brings the copper cations to within 3.43 Å of each other. A schematic representation of the structure of **4** is displayed in Scheme 4.



Scheme 4. A schematic representation of **4**

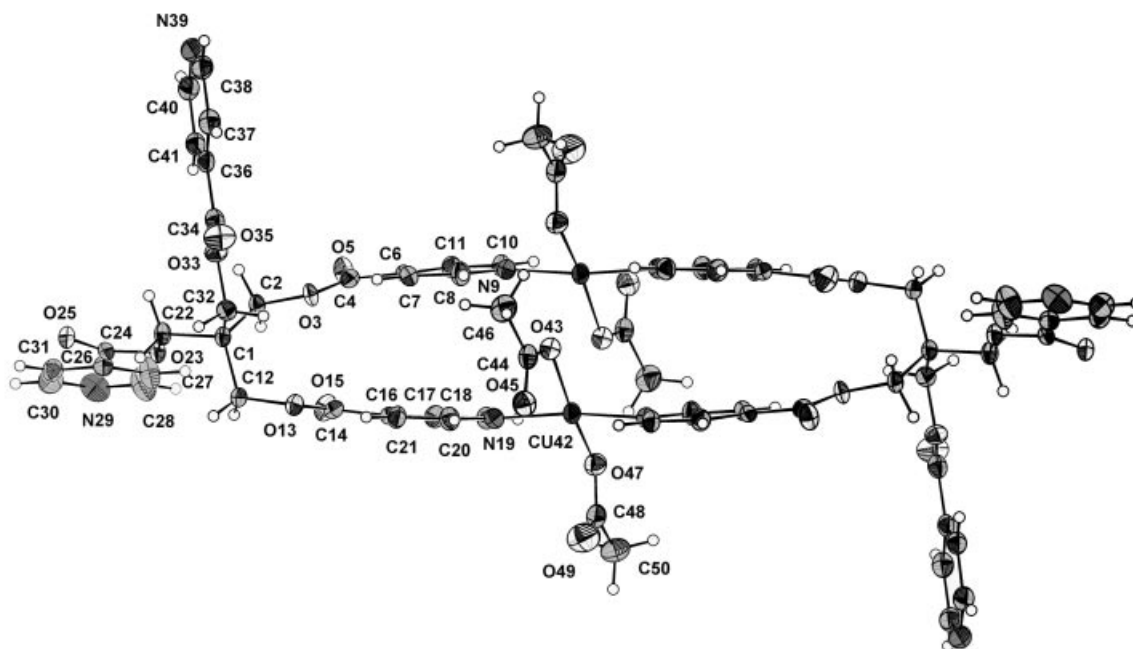


Figure 6. A plot with thermal ellipsoids shown at the 50% probability level for **4**, with the numbering of the non-hydrogen atoms of the asymmetric unit. The solvent water molecules are excluded

Several hydrogen bonds and other weak interactions such as $\text{CH}\cdots\pi$ and $\pi\cdots\pi$ interactions are involved in the packing of **4**. Despite the available coordinating sites of the terminal nitrogen atoms, only two arms of each TINM are coordinated. Although the use of copper acetate instead of copper nitrate is the only difference between the synthesis of the 3D MOF in our previous work^[29] and the synthesis of **4**, a dimeric rather than a polymeric complex is obtained. A 3D MOF is not formed because the coordination geometry around the copper cation is square-planar. Despite the availability of nitrogen atoms for coordination, the complex remains a dimer, and does not form chains as in structures **2** and **3**. The multiple weak intermolecular interactions between the uncomplexed pyridyl moieties of the dimers could possibly be the reason for the lack of strand or layer formation. A strong hydrogen-bond is formed between the uncoordinated nitrogen atom N29 and a water molecule ($\text{DH}\cdots\text{A}$: 2.017 Å, $\text{D}-\text{H}-\text{A}$: 171.3°). The other uncoordinated nitrogen atom N39 is blocked since it intertwines with the ends of neighboring molecules (Figure 7).

The completely different architectures of the layer structure of **3** and the dimeric structure of **4** can be explained by the greater bridging ability of the nitrate anion relative to that of the acetate anion. Since the nitrate anions in the previously reported structures do not participate significantly in the formation of the framework,^[29] the difference between these 3D MOF structures and **4** is probably due to polymorphism, rather than differences between the acetate and nitrate anions.

TGA Studies: As expected, the TGA studies do not show the removal of solvents before high temperatures were reached. In complex **1**, a weight loss of 15% is observed before decomposition at 280 °C. This approximately corresponds to the eight uncoordinated water molecules in the lattice (Figure 8). The TGA curve of **2** reveals stepwise decomposition of the structure beginning at 260 °C, and for complex **3**, at 280 °C. In complex **3**, the only solvent molecule is coordinated by the silver cation, thus its removal

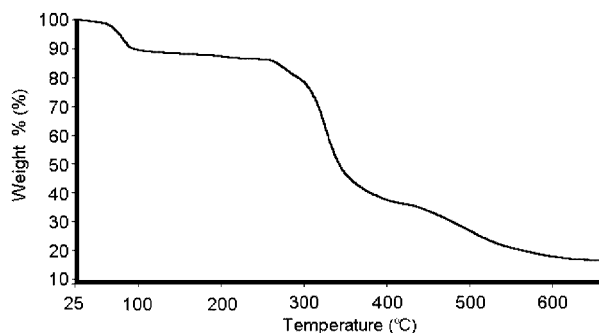


Figure 8. The TGA curve for **1**

results in the rapid collapse of the structure. In the TGA analysis of **4**, no intermediate products are seen. The decomposition occurs in one step, in contrast with the TGA results of the MOFs **1**, **2** and **3**, all of which display stepwise thermal decomposition.

Conclusions

The pseudo 3D MOF structure **1** is in fact a 2D MOF since it does not have an infinite third dimension. The thickness of the layers in **1** is 2.1 nm. In spite of the octahedral coordination geometry around the copper cations and the skewed tetrahedral conformation of the pyridyl moieties of TNM, a 3D MOF is not formed. This is because the branching from the metal center is directed only towards the center of the layer from the metal centers on both the top and bottom of the layer. This is probably due to the lack of space for the sulfate anion. The relatively short arms of TNM, and the large size and long bond length of the sulfate anion relative to the anions used in the synthesis of the 3D MOFs with copper and TNM/TINM ligands in our previous study, prevent the formation of a 3D MOF with suitable cavities for the sulfate anions.^[29] Ad-

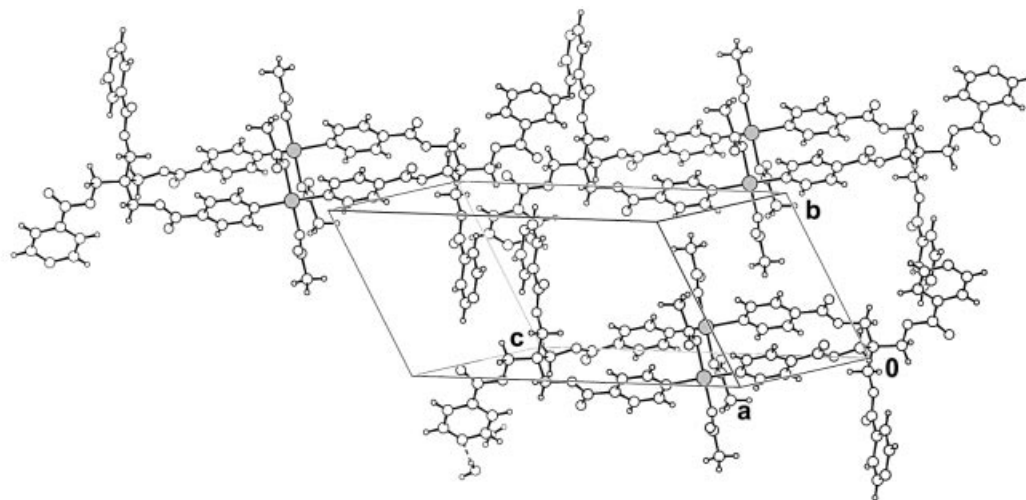


Figure 7. Three dimers of **4** showing the unit cell and the hydrogen-bond between water and N29

ditionally, due to the *meta*-position of the nitrogen atom, the TNM ligands are incapable of aligning in a co-planar manner to the equatorial metal coordination plane, and therefore are unable to assume a conformation similar to that of the ligands in the 3D MOFs in our previous study.

Structure **2**, a polymeric complex of zinc chloride and TNM, is composed of infinite, flat, linear chains of TINM ligands linked by zinc cations. Despite the potential ability of **2** and **3** to form 2D layers through metal–nitrogen bonds alone, only 1D chain structures are obtained from these interactions. The formation of 3D MOFs is prevented because the zinc cation in **2** has only two coordination sites for the ligand, and the pyridyl moieties of the TNM are paired, i.e. they are not tetrahedrally oriented. In contrast with the nitrate anions in **3**, the chloride anion in **2** is incapable of promoting layer formation by creating links between individual chains. The layers of chains in **2** are tightly packed, and each layer of chains forms a 60° angle with its neighbors. A probable explanation for not obtaining 2D layers (besides those created by the anion bridging in **3**) is the low packing efficiency of these grid structures. The high complementarity requirements for interpenetrating frameworks may not be fulfilled.

The $\pi\cdots\pi$ interactions between the pyridyl rings of adjacent arms are probably the driving force for the formation of the structure **3**. A polymeric chain of the TINM ligands, with paired pyridyl moieties coordinated by the silver cations in one dimension is formed. However, by coordinating three silver cations, the nitrate anions create a link between the chains, and thereby form a 2D layer structure with a thickness of 13.2 Å. The cyclic dimeric metal complex formed between TINM and copper acetate, structure **4**, provides interesting possibilities for heterometallic complexation. This is because the remaining, uncomplexed four arms of the dimer are available for further coordination. The completely different architecture of **4** with respect to previous structures^[29] with the nitrate anion instead of the acetate anion probably arises as a result of polymorphism.

Experimental Section

Materials and Measurements: All commercially available chemicals were of reagent grade and used as received without further purification. TINM and TNM were synthesized as previously reported.^[34] The purity of the complexes was confirmed by elemental analysis. TGA experiments were carried out at a heating rate of 5 °C/min under nitrogen using a Perkin–Elmer TGA 7 instrument. The elemental analyses were performed at the University of Joensuu using CE-Instruments EA1110. The elemental analyses revealed a loss of solvent for structure **1**, and some solvent residuals for **2** and **4**, thus giving inaccurate results for the chemical compositions. Therefore, only the results for the elemental analyses of **1** and **3** are presented. The complexes were not vacuum dried before elemental analysis, so as to avoid decomposition.

Preparation of the Complexes [Cu(TNM)(SO₄)(H₂O)₂](MeOH)₂(H₂O)₈ (1**):** CuSO₄·5H₂O (22.4 mg, 89.8 µmol) in water (10 mL) was added to TINM (50 mg, 89.8 µmol) dissolved in MeOH (30 mL). The solution was evaporated slowly, and the crys-

talline solid was collected from the solution before complete evaporation of the solvents. The solid was washed with water and dried in air. Yield 54.6% (46.7 mg). C₃₁H₄₄CuN₄O₂₄S₁ – (8H₂O + 2MeOH), [Cu(TNM)(SO₄)(H₂O)₂]: calcd. C 46.3, H 3.8, N 7.5; found C 46.2, H 3.6, N 7.5.

[Zn₂(TNM)Cl₄](MeCN)_{2/3}(H₂O)_{1/3} (2**):** ZnCl₂ (24.5 mg, 89.8 µmol) in water (10 mL) was added to TNM (50 mg, 89.8 µmol) dissolved in MeCN (35 mL). The solution was evaporated slowly, and the crystalline solid was collected from the solution before complete evaporation of the solvents. The solid was washed with water and dried in air. Yield 100% (76.8 mg).

[Ag₂(TINM)(NO₃)₂(H₂O)] (3**):** AgNO₃ (30.5 mg, 89.8 µmol) in water (10 mL) was added to TINM (50 mg, 89.8 µmol) dissolved in MeCN (30 mL). The solution was evaporated slowly, and the crystalline solid was collected from the solution before complete evaporation of the solvents. The solid was washed with water and dried in air. Yield 100% (82.1 mg). C₂₉H₂₆Ag₂N₆O₁₅: calcd. C 38.1, H 2.9, N 9.2; found: C 38.9, H 2.9, N 9.2.

[Cu(TINM)(O₂CCH₃)₂](H₂O)₄ (4**):** Cu(O₂CCH₃)₂·3H₂O (16.3 mg, 89.8 µmol) in water (5 mL) was added to TINM (50 mg, 89.8 µmol) dissolved in MeOH (30 mL). The solution was evaporated slowly, and the blue crystalline solid was collected from the solution before complete evaporation of the solvents. The solid was dried in air. Yield 20.7% (15.1 mg).

X-ray Diffraction: The single crystal X-ray diffraction was performed using a Nonius–KappaCCD diffractometer with graphite-monochromatized Mo-*K*_α (λ = 0.71073 Å) radiation. Collect software was used for the measurement and DENZO-SMN^[35] for the processing of the data. The structures were solved and refined by full-matrix least-squares on *F*² using the WinGX-software package which utilizes the SHELXS-97 and SHELXL-97 modules.^[36–38] Hydrogen atoms were refined using a riding model. Empirical absorption correction was performed for complexes **1**, **2**, and **3**. The graphic presentations of the structures were created with the software package Diamond.^[39] CCDC-206599, -206600, -206601 and -206602 contain the supplementary crystallographic data for this paper. These data can be obtained free of charge on application to The Director, CCDC, 12 Union Road, Cambridge CB2 1EZ, UK [Fax: (internat.) +44-1223- 336-033; E-mail: deposit@ccdc.cam.ac.uk].

Acknowledgments

K. N. thanks the Graduate School of Bioorganic Chemistry for financial support. K. R. thanks the Finnish Academy (proj. no. 777871) for financial support.

- [1] M.-L. Tong, B.-H. Ye, J.-W. Cai, X.-M. Chen, S. W. Ng, *Inorg. Chem.* **1998**, 37, 2645.
- [2] O.-S. Jung, Y. J. Kim, Y.-A. Lee, J. K. Park, H. K. Chae, *J. Am. Chem. Soc.* **2000**, 122, 9921.
- [3] D. Williams, B. Pleune, J. Kouvetakis, M. D. Williams, R. A. Andersen, *J. Am. Chem. Soc.* **2000**, 122, 7735.
- [4] G. J. Halder, C. J. Kepert, B. Maoubaraki, K. S. Murray, J. D. Cashion, *Science* **2002**, 298, 1762.
- [5] M. Eddaoudi, J. Kim, N. Rosi, D. Vodak, J. Wachter, M. O’Keefe, O. M. Yaghi, *Science* **2002**, 295, 469.
- [6] X. Wang, M. Simard, J. D. Wuest, *J. Am. Chem. Soc.* **1994**, 116, 12119.

- [7] G. R. Desiraju, *Angew. Chem. Int. Ed. Engl.* **1995**, *34*, 2311.
- [8] S. Kheradmandan, H. W. Schmalke, H. Jacobsen, O. Blacque, T. Fox, H. Berke, M. Gross, S. Decurtins, *Chem. Eur. J.* **2002**, *8*, 2526.
- [9] P. Jensen, S. R. Batten, B. Moubaraki, K. S. Murray, *J. Chem. Soc., Dalton Trans.* **2002**, 3712.
- [10] S. Muthu, J. H. K. Yip, J. J. Vittal, *J. Chem. Soc., Dalton Trans.* **2002**, 4561.
- [11] I. Ino, J. C. Zhong, M. Munakata, T. Kuroda-Sowa, M. Maekawa, Y. Suenaga, Y. Kitamori, *Inorg. Chem.* **2000**, *39*, 4273.
- [12] O. Ermer, L. Lindenberg, *Helv. Chim. Acta* **1991**, *74*, 825.
- [13] M. Simard, D. Su, J. D. Wuest, *J. Am. Chem. Soc.* **1991**, *113*, 4696.
- [14] D. Venkatamaran, S. Lee, J. Zhang, J. S. Moore, *Nature* **1994**, *371*, 591.
- [15] H. Sauriat-Dorizon, T. Maris, J. D. Wuest, *J. Org. Chem.* **2003**, *68*, 240.
- [16] K. Biradha, K. V. Domasevitch, B. Moulton, C. Seward, M. J. Zaworotko, *Chem. Commun.* **1999**, 1327.
- [17] K. A. Hirsch, S. R. Wilson, J. S. Moore, *Inorg. Chem.* **1997**, *36*, 2960.
- [18] M. A. Withersby, A. J. Blake, N. R. Champness, P. A. Cooke, P. Hubberstey, A. L. Realf, S. J. Teat, M. Schröder, *J. Chem. Soc., Dalton Trans.* **2000**, 3261.
- [19] M.-L. Tong, S.-L. Zheng, X.-M. Chen, *Polyhedron* **2000**, *19*, 1809.
- [20] S. Muthu, J. H. K. Yip, J. J. Vittal, *J. Chem. Soc., Dalton Trans.* **2002**, 4561.
- [21] K. A. Hirsch, S. R. Wilson, J. S. Moore, *Chem. Commun.* **1998**, 13.
- [22] O. M. Yaghi, H. Li, *J. Am. Chem. Soc.* **1995**, *117*, 10401.
- [23] M. J. Plater, M. R. St J. Foreman, J. M. S. Skakle, *Cryst. Eng.* **2001**, *4*, 293.
- [24] D. M. L. Goodgame, D. A. Grachvogel, A. J. P. White, D. J. Williams, *Inorg. Chem.* **2001**, *40*, 6180.
- [25] B. F. Hoskins, R. Robson, *J. Am. Chem. Soc.* **1990**, *112*, 1546.
- [26] F. Gröhn, G. Kim, B. J. Bauer, E. J. Emis, *Macromolecules* **2001**, *34*, 2179.
- [27] G. M. J. Schmidt, *Pure Appl. Chem.* **1971**, *27*, 647.
- [28] J. Fan, H.-F. Zhu, T.-a. Okamura, W.-Y. Sun, W.-X. Tang, N. Ueyama, *Inorg. Chem.* **2003**, *42*, 158.
- [29] K. Nättinen, K. Rissanen, *Inorg. Chem.* **2003**, *42*, 5126.
- [30] L. Carlucci, G. Ciani, D. Proserpio, S. Rizzato, *CrystEngComm* **2002**, *4*, 121.
- [31] C. Janiak, *Angew. Chem. Int. Ed. Engl.* **1997**, *36*, 1431.
- [32] G. B. Gardner, D. Venkatamaran, J. F. Moore, S. Lee, *Nature* **1995**, *374*, 792.
- [33] J. Kim, B. Chen, T. M. Reineke, H. Li, M. Eddaoudi, D. B. Moler, M. O'Keeffe, O. M. Yaghi, *J. Am. Chem. Soc.* **2001**, *123*, 8239.
- [34] K. Nättinen, K. Rissanen, *Cryst. Growth Des.* **2003**, *3*, 339.
- [35] Z. Otwinowski, W. Minor, *Methods in Enzymology, Macromolecular Crystallography, Part A*, (Eds.: C. W. Carter, Jr., M. Sweet), **1997**, pp. 307–326, Academic Press, New York.
- [36] L. J. Farrugia, *J. Appl. Cryst.* **32**, 837.
- [37] G. M. Sheldrick, *Acta Crystallogr., Sect. A* **1990**, *46*, 467.
- [38] G. M. Sheldrick, SHELXL-97 – A program for crystal structure refinement, **1997**, University of Göttingen, Germany.
- [39] DIAMOND – Visual Crystal Structure Information System, Prof. Dr. G. Bergerhoff, Gerhard-Domagk-Str. 1, 53121 Bonn, Germany.

Received May 12, 2003

Early View Article

Published Online October 2, 2003